Available online at www.sciencedirect.com
SCIENCE DIRECT®
Journal of Process Control 14 (2004) 837–852
JOURNAL OF PROCESS CONTROL
www.elsevier.com/locate/jprocont

On-line state and parameter estimation of EPDM polymerization reactors using a hierarchical extended Kalman filter

Rujun Li [a], Armando B. Corripio [a], Michael A. Henson [b,*], Michael J. Kurtz [c]

[a] Gordon A. and Mary Cain Department of Chemical Engineering, Louisiana State University Baton Rouge, LA 70803-7303, USA
[b] Department of Chemical Engineering, University of Massachusetts, Amherst, MA 01003-3110, USA
[c] ExxonMobil Chemical Company, Baton Rouge, LA 70805-3359, USA

Received 18 August 2003; received in revised form 3 March 2004; accepted 3 March 2004

Abstract

A hierarchical extended Kalman filter (EKF) design is proposed to estimate unmeasured state variables and key kinetic parameters in a first principles model of a continuous ethylene–propylene–diene polymer (EPDM) reactor. The estimator design is based on decomposing the dynamic model into two subsystems by exploiting the triangular model structure and the different sampling frequencies of on-line and laboratory measurements directly related to the state variables of each subsystem. The state variables of the first subsystem are reactant concentrations and zeroth-order moments of the molecular weight distribution (MWD). Unmeasured state variables and four kinetic parameters systematically chosen to reduce bias are estimated from frequent and undelayed on-line measurements of the ethylene, propylene, diene and total polymer concentrations. The state variables of the second subsystem are first-order moments of the MWD. Given state and parameters estimates from the first subsystem EKF, the first-order moments and three non-stationary parameters added to the model for bias reduction are estimated from infrequent and delayed laboratory measurements of the ethylene and diene contents and number average molecular weight of the polymer. Simulation tests show that the hierarchical EKF generates satisfactory estimates even in the presence of measurement noise and plant/model mismatch.

Keywords: State estimation; On-line parameter estimation; Extended Kalman filter; Polymerization reactors

1. Introduction

Ethylene–propylene (EPM) copolymers and ethylene–propylene–diene (EPDM) terpolymers are used extensively in the automotive, construction and agricultural industries [9,37]. In 1995 the domestic production of these rubbers was almost 400,000 metric tons [1]. EPM and EPDM are commonly manufactured via a solution polymerization process in which a continuous stirred tank reactor based on Ziegler–Natta catalyst technology is the key unit operation. Product quality is determined primarily by the Mooney viscosity (a measure of molecular weight) and the relative contents of the ethylene, propylene and diene monomers in the polymer. Stable reactor operation is required to minimize off-specification polymer and to maximize production rates. EPDM reactors are commonly monitored using simple statistical quality control techniques in which laboratory measurement are compared to target product properties. Due to the high cost and manual nature of laboratory analysis, the product quality measurements are available infrequently and contain significant time delays. As a result, purely statistical techniques are unlikely to yield an adequate characterization of the current reactor state.

A more sophisticated approach for polymerization reactor monitoring involves the combination of a kinetic model with available measurements to infer the current process state [2,3,13,15,27,38,40]. Although conceptually appealing, the state estimation approach is difficult to implement an industrial environment because: (i) a nonlinear estimation strategy is required to accurately track reactor changes over a wide range of operating conditions; (ii) on-line and laboratory measurements with widely varying sampling frequencies and analysis delays must be integrated; and (iii) the complexity of the

* Corresponding author. Tel.: +1-413-545-3481; fax: +1-413-545-1647.
E-mail address: henson@ecs.umass.edu (M.A. Henson).

0959-1524/$ - see front matter © 2004 Elsevier Ltd. All rights reserved.
doi:10.1016/j.jprocont.2004.03.002

polymerization dynamics invariably leads to significant parametric and structural plant/model mismatch. Multirate nonlinear state estimation strategies that address the first two issues have been developed for particular polymerization reactors [10,25,26,28,39]. Available multirate methods are direct extensions of single rate techniques in the sense that on-line and laboratory measurements are integrated into a single estimator designed using the complete reactor model.

We pursue an alternative nonlinear estimation strategy that exploits the EPDM model structure as well as the multirate nature of the available measurements. The triangular structure of the mass balance and moment equations allows the reactor model to be decomposed into two distinct subsystems. The first subsystem contains differential equations for the reactant concentrations and zeroth-order moments of the molecular weight distribution (MWD) and is completely independent of the second subsystem. By contrast, the second subsystem consisting of differential equations for the first-order MWD moments is affected by the first subsystem. Rather than formulate a single estimator that processes all the measurements, we propose a hierarchical approach in which the on-line measurements are used as inputs to a first estimator and the laboratory measurements and estimates from the first subsystem are used as inputs to a second estimator. As compared to existing nonlinear multirate estimation techniques, advantages of the proposed method include: (1) reduced computational requirements and improved numerical stability resulting from decomposition of a single large estimator into two smaller estimators; and (2) easier implementation and reduced maintenance requirements owing to the modular nature of the hierarchical estimators.

A typical EPDM plant produces a range of polymer grades that differ with respect to catalyst system, diene monomer type and/or product quality targets. Determination of kinetic parameter values from literature data and specialized laboratory experiments is not feasible for each polymer in the gradeslate. A common approach for reducing estimation bias resulting from parametric and structural modeling errors is to estimate a few key model parameters along with the unmeasured state variables [13,19,36]. The success of combined state/parameter estimation depends critically on proper selection of the adjustable model parameters [28,36]. Rather than heuristically choose the estimated parameters based on process knowledge, we utilize a systematic parameter selection method previously developed by our group [17] that exploits the available kinetic model. The steady-state parameter-measurement sensitivity matrix is used to achieve an acceptable compromise between the magnitude and uniqueness of parameter effects on the measured outputs. Unlike alternative methods that simply allow screening of predetermined parameter sets [35], our method yields an explicit ranking of the candidate parameters according to their usefulness for reducing estimation bias.

A wide variety of nonlinear state estimation techniques are potentially applicable to the EPDM problem. Nonlinear state estimators commonly used for process control applications can be classified as extended Luenberger observers [3,38], extended Kalman filters [24,34] and nonlinear receding horizon estimators [29,30]. While extended Luenberger observers are most suitable for theoretical analysis, they typically require nonlinear coordinate transformations that are difficult to construct for complex models and that raise concerns about numerical stability in an industrial environment subject to significant noise and frequent disturbances. A major advantage of nonlinear receding horizon estimators is the ability to enforce constraints on the estimated variables. Because constrained estimates are generated by solving a non-convex nonlinear program at each sampling period, the computational overhead can be prohibitive for complex models such as those required to describe EPDM reactor dynamics. The hierarchical estimation strategy proposed in this paper is based on the extended Kalman filter (EKF) [11,12,24] because: (1) restrictive assumptions on the model structure required in other nonlinear state estimation techniques [5,14,23,41] are not necessary; (2) measurements with different sampling frequencies and analysis delays can be handled [10,25,26,28,39]; and (3) on-line computational demands are much less than for nonlinear receding horizon estimators [22,29,30].

The proposed estimation strategy is particularly well suited for application to industrial EPDM reactors. Although applicable to a wide range of on-line estimation problems, the parameter selection procedure ensures the adjustment of kinetic parameters that minimize estimation bias [17]. By utilizing extended Kalman filtering for combined state and parameter estimation, ill-conditioning problems associated with variable transform methods [5] and the large computational requirements of optimization based methods [29] are avoided. Model decomposition allows sequential design of the two subsystem estimators, thereby reducing trial-and-error tuning of the covariance matrices, improving numerical stability and simplifying on-line implementation as compared to existing multirate EKF schemes [26]. Another advantage of the hierarchical structure is that the first subsystem estimator is not affected by disabling the second subsystem estimator in the event that laboratory measurements become unavailable or maintenance is required.

The remainder of the paper is organized as follows. The EPDM kinetic model and the assumed on-line and laboratory measurements are discussed in Section 2. Section 3 contains a detailed description of estimator design including model decomposition into two subsystems, selection of the estimated parameters and for-

mulation of the hierarchical EKFs. The simulated performance of the hierarchical estimator in the presence of parametric and structural modeling errors is presented and discussed in Section 4. A brief summary and the major conclusions are presented in Section 5.

2. EPDM kinetic model

We consider a solution polymerization process in which EPDM is produced in a continuous stirred tank reactor. The feed to the reactor consists of the three monomers, solvent (hexane or methyl chloride), catalysts (a transition metal halide catalyst and an oganometallic co-catalyst) and chain-transfer agent (usually hydrogen). The reactor model is based on a kinetic mechanism that describes the major reactions involved in initiation, propagation, termination and transfer of polymer chains. We utilize the kinetic mechanism of Cozewith [6] shown in Table 1. The basic reaction steps are: (i) formation of an active catalyst species (C_2) from the catalyst (C_1) and co-catalyst (Al); (ii) deactivation of the catalyst with various poisons such as diene monomer (M_3) to form dead catalyst species (D); (iii) initiation of a growing polymer chain by the reaction of active catalyst with ethylene monomer (M_1) or propylene monomer (M_2); (iv) propagation of a polymer chain by the addition of a monomer unit to the growing chain; (v) termination of polymer chain growth by the transformation of a growing chain to a dead chain; and (vi) transfer of the active catalyst from a growing polymer chain to a new polymer chain by the action of chain transfer agents such as hydrogen (H_2). Alternative EPDM kinetic schemes [7,26] differ from the mechanism in Table 1 with respect to particular chain initiation, propagation, termination and transfer reactions. The notation P_{ijk} and U_{ijk} is used to represent ethylene ended growing and dead chains, respectively, with a total number of i ethylene units, j propylene units, and k diene units. Two types of propylene ended chains (Q_{ijk}, V_{ijk}) and diene ended chains (R_{ijk}, W_{ijk}) are labeled analogously. Each reaction j has an associated rate constant k_j whose value must be obtained from the literature or estimated from available data.

Table 1
EPDM kinetic mechanism

Type	Reaction	Rate constant
1. Catalyst activation	$C_1 \rightarrow C_2$	k_a
2. Catalyst deactivation	$C_1 \rightarrow D$	k_x
	$C_1 + M_3 \rightarrow D$	k_{x3}
3. Chain initiation	$C_2 + M_1 \rightarrow P_{100}$	k_{i1}
	$C_2 + M_2 \rightarrow Q_{010}$	k_{i2}
4. Chain propagation	$P_{ijk} + M_1 \rightarrow P_{(i+1)jk}$	k_{11}
	$P_{ijk} + M_2 \rightarrow Q_{i(j+1)k}$	k_{12}
	$P_{ijk} + M_3 \rightarrow R_{ij(k+1)}$	k_{13}
	$Q_{ijk} + M_1 \rightarrow P_{(i+1)jk}$	k_{21}
	$Q_{ijk} + M_2 \rightarrow Q_{i(j+1)k}$	k_{22}
	$R_{ijk} + M_1 \rightarrow P_{(i+1)jk}$	k_{31}
5. Chain termination		
Spontaneous	$P_{ijk} \rightarrow U_{ijk}$	k_t
	$Q_{ijk} \rightarrow V_{ijk}$	k_t
	$R_{ijk} \rightarrow W_{ijk}$	k_t
With propylene	$P_{ijk} + M_2 \rightarrow U_{ijk}$	k_{t2}
	$Q_{ijk} + M_2 \rightarrow V_{ijk}$	k_{t2}
	$R_{ijk} + M_2 \rightarrow W_{ijk}$	k_{t2}
With diene	$P_{ijk} + M_3 \rightarrow U_{ijk}$	k_{t3}
	$Q_{ijk} + M_3 \rightarrow V_{ijk}$	k_{t3}
	$R_{ijk} + M_3 \rightarrow W_{ijk}$	k_{t3}
6. Chain transfer		
With hydrogen	$P_{ijk} + H_2 \rightarrow U_{ijk} + C_2$	k_{tr1}
	$Q_{ijk} + H_2 \rightarrow V_{ijk} + C_2$	k_{tr1}
	$R_{ijk} + H_2 \rightarrow W_{ijk} + C_2$	k_{tr1}
With co-catalyst	$P_{ijk} + Al \rightarrow U_{ijk} + P_{100}$	k_{tr}
	$Q_{ijk} + Al \rightarrow V_{ijk} + P_{100}$	k_{tr}
	$R_{ijk} + Al \rightarrow W_{ijk} + P_{100}$	k_{tr}
With propylene	$P_{ijk} + M_2 \rightarrow U_{ijk} + Q_{010}$	$k_{tr_{M2}}$
	$Q_{ijk} + M_2 \rightarrow V_{ijk} + Q_{010}$	$k_{tr_{M2}}$
	$R_{ijk} + M_2 \rightarrow W_{ijk} + Q_{010}$	$k_{tr_{M2}}$

The reactor model consists of dynamic balance equations for the reacting species and various MWD moments. Overall mass and energy balances are not included because EPDM reactors are operated at constant volume and temperature except for grade transitions which are not considered in this paper. Because the available measurements discussed below are not related to second-order MWD moments, the model only includes moments up to first order. In the absence of multiple catalyst sites and/or polymer cross-linking, this simplification is reasonable because the steady-state polydispersity is identically two for any operating conditions [6,7]. The resulting dynamic model consists of 14 nonlinear ordinary differential equations (ODEs) for the seven reacting species (ethylene, propylene and diene monomers, inactive and active catalysts, co-catalyst and hydrogen), four zeroth-order moments (concentrations of ethylene ended chains P_0, propylene ended chains Q_0, diene ended chains R_0 and dead chains B_0) and three first-order bulk moments (total concentrations of ethylene λ_{100}, propylene λ_{010} and diene λ_{001} in the polymer chains).

Appendix A.1 contains the complete set of model equations where C denotes a molar concentration, F is the volumetric feed flow rate, V is the constant reactor volume, and the subscript 'f' denotes a feed property. The chain transfer reaction involving the aluminum alkyl co-catalyst is assumed to be proportional to the excess co-catalyst that remains following the formation of the active catalyst species. Nominal parameter values for the EPDM grade studied are listed in Table 2 [17]. Each parameter value has been scaled to have roughly the same order of magnitude. The dynamic model equations can be written in the general form:

$$\dot{x} = f(x, u, \theta) \tag{1}$$

Table 2
Scaled reaction rate constants

Parameter	Value	Parameter	Value
k_a	0.3663	k_{21}	0.6410
k_x	0	k_{22}	3.0037
k_{x_2}	0	k_{31}	1.2418
k_{x_3}	0.9890	k_t	0.5604
k_{i1}	1.8315	k_{t_2}	0.7839
k_{i2}	1.8315	k_{t_3}	0
k_{11}	0.4212	k_{tr}	0
k_{12}	0.6886	k_{tr_1}	1.7582
k_{13}	0.4139	$k_{tr_{M_2}}$	1

where $x \in R^{14}$ is the state vector, θ is a vector of estimated parameters to be defined later, and $u \in R^6$ is a vector of feed concentrations used for process excitation:

$$u = \begin{bmatrix} C_{M_{1,f}} & C_{M_{2,f}} & C_{M_{3,f}} & C_{C_{1,f}} & C_{Al,f} & C_{H_{2,f}} \end{bmatrix}^{\mathrm{T}} \tag{2}$$

The reactor model is completed by specifying the measurements along with their sampling frequencies and analysis delays. Frequent and undelayed measurements of the ethylene concentration (C_{M_1}), propylene concentration (C_{M_2}), diene concentration (C_{M_3}) and total polymer concentration (λ_0) are assumed to be available. ExxonMobil work demonstrates that such on-line measurements can be obtained via a combination of Fourier transform near infrared (FTNIR) spectroscopy and multivariate statistical analysis of the resulting spectra [21]. A sampling time of six minutes is necessary to flush the probe following each sample and mitigate fouling problems. The total polymer concentration is related to the zeroth-order moments as follows:

$$\lambda_0 = P_0 + Q_0 + R_0 + B_0 \tag{3}$$

Infrequent and delayed measurements of the polymer ethylene content (X_{M_1}), diene content (X_{M_3}) and number average molecular weight ($\overline{M}_n$) are assumed to be provided by laboratory analysis. While not measured directly, $\overline{M}_n$ can be inferred from the measured Mooney viscosity (M_L) using the empirical equation:

$$M_L = a(\overline{M}_n/1000)^b \tag{4}$$

where a and b are grade dependent constants. ExxonMobil currently analyzes polymer samples every two hours immediately following grade transitions and every four hours during normal operation. Each measurement is delayed by approximately one hour due to sampling, laboratory analysis and transmission of results. Consequently, we assume the three laboratory measurements are available every two hours with a one hour delay. These measurements are related to the first-order moments as follows [20,31]:

$$X_{M_1} = \frac{M_{w_1}\lambda_{100}}{M_{w_1}\lambda_{100} + M_{w_2}\lambda_{010} + M_{w_3}\lambda_{001}} \tag{5}$$

$$X_{M_3} = \frac{M_{w_3}\lambda_{001}}{M_{w_1}\lambda_{100} + M_{w_2}\lambda_{010} + M_{w_3}\lambda_{001}} \tag{6}$$

$$\overline{M}_n = \frac{M_{w_1}\lambda_{100} + M_{w_2}\lambda_{010} + M_{w_3}\lambda_{001}}{\lambda_0} \tag{7}$$

where M_{w_1}, M_{w_2} and M_{w_3} are the molecular weights of ethylene, propylene and diene, respectively.

3. Design of the hierarchical extended Kalman filter

The EPDM dynamic model has a triangular structure common to other types of polymerization reactor models in which a first subsystem comprised of reactant concentrations and zeroth-order MWD moments is decoupled from a second subsystem consisting of first-order MWD moments. An EKF that receives frequent and undelayed on-line measurements of the ethylene, propylene, diene and total polymer concentrations is used to estimate reactant concentrations and zeroth-order MWD moments as well as four kinetic parameters systematically chosen to reduce bias in the first subsystem. The first subsystem estimates serve as inputs to a second EKF that generates estimates of the first-order MWD moments and three additive parameters from infrequent and delayed laboratory measurements of the ethylene and diene contents and number average molecular weight of the polymer. This hierarchical formulation allows the two EKFs to be designed sequentially and the second subsystem correction term to be utilized only when laboratory measurements become available. Our goal is to develop a nonlinear state estimator strategy that is implementable in an industrial environment rather than theoretical analysis of estimator convergence under idealized conditions. The interested reader is referred to other papers for detailed stability analysis of the EKF [4,18,32,33].

3.1. Model decomposition

The proposed decomposition exploits the triangular structure of the EPDM model and the different sampling frequencies of the available measurements. The first subsystem is represented as

$$\begin{aligned} \dot{x}_1(t) &= f_1[x_1(t), u(t), \theta_1] \\ \dot{\theta}_1(t) &= 0 \\ y_1(kh_1) &= h_1[x_1(kh_1)] = C_1 x_1(kh_1) \end{aligned} \tag{8}$$

where the state variables $x_1 = [C_{M_1}\ C_{M_2}\ C_{M_3}\ C_{C_1}\ C_{C_2}\ C_{Al}\ C_{H_2}\ P_0\ Q_0\ R_0\ B_0]^{\mathrm{T}} \in R^{11}$ are continuous functions of time and the on-line measurements $y_1 = [C_{M_1}\ C_{M_2}\ C_{M_3}\ \lambda_0]^{\mathrm{T}} \in R^4$ are discrete signals with a sampling period of $h_1 = 6$ min and no analysis delay. The kinetic parameters θ_1 chosen for on-line estimation are appended to the model as additional unmeasured state

variables. A systematic procedure for selecting these parameters to reduce estimation bias is discussed below. The second subsystem is written as

$$\begin{aligned}\dot{x}_2(t) &= f_2[x_1(t), x_2(t), u(t), \theta_1] + \theta_2 \\ \dot{\theta}_2(t) &= 0 \\ y_2(kh_2) &= h_2[x_1(kh_2 - t_2), x_2(kh_2 - t_2)]\end{aligned} \tag{9}$$

where the state variables $x_2 = [\,\lambda_{100} \quad \lambda_{010} \quad \lambda_{001}\,]^{\mathrm{T}} \in R^3$ are continuous functions of time and the laboratory measurements $y_2 = [\,X_{M_1} \quad X_{M_2} \quad \overline{M}_n\,]^{\mathrm{T}} \in R^3$ are discrete signals with a sampling period $h_2 = 2$ h and analysis delay $t_2 = 1$ h. The parameters θ_2 added to the model to reduce estimation bias are discussed below. The sampling intervals of the on-line and laboratory measurement are related as: $N = \frac{h_2}{h_1} = 20$.

3.2. Selection of estimated parameters

The subsystem models (8) and (9) used for nonlinear estimation are formulated by considering selected parameters as unmeasured state variables. On-line parameter estimation is necessary to account for modeling errors that result from limited process understanding, the introduction of simplifying assumptions and inaccurate parameter values due to limited experimental data. The objective is to select the parameters such that estimation bias is minimized and localized to the least important state variables. To ensure that the parameters are observable and that bias is eliminated in each measured variable, the number of estimated parameters must be equal to the number of measurements [13,34]: $\theta_1 \in R^4$ and $\theta_2 \in R^3$.

The first subsystem is comprised of balance equations for the reacting species and the zeroth-order MWD moments. The kinetic mechanism in Table 1 involves a total of 18 rate constants k_j, four of which are identically zero for the specific grade studied (see Table 2). A systematic approach for selecting the four estimated parameters θ_1 from the remaining set of 14 rate constants is necessary to achieve a suitable tradeoff between the following factors:

1. A parameter may have a very weak effect on the measured outputs. Successful estimation of such a weakly identifiable parameter is unlikely because its effect cannot be accurately quantified.
2. The effects of certain parameters on the measured outputs may be almost linearly dependent. Successful estimation of such parameter sets is unlikely because the individual parameter effects cannot be distinguished.

The presence of parameters with weak and/or nearly linearly dependent effects on the measured outputs often leads to estimator convergence problems [17].

We recently developed a systematic technique for selecting parameters for off-line estimation that explicitly addresses the tradeoff between the magnitude and uniqueness of parameter effects [17]. The recursive parameter selection algorithm used for on-line estimation is summarized in Appendix A.2. As discussed in the original reference [17], the algorithm selects the following kinetic parameters for the first subsystem: k_a, k_{tr1}, k_{13} and k_{11}. The parameters $\theta_1 = [\,s_a \quad s_{tr1} \quad s_{13} \quad s_{11}\,]^{\mathrm{T}}$ actually included in the estimator design model (8) are defined as follows:

$$k_a^* = s_a k_a, \quad k_{tr_1}^* = s_{tr_1} k_{tr_1}, \quad k_{13}^* = s_{13} k_{13}, \quad k_{12}^* = s_{11} k_{11} \tag{10}$$

where k_j represents the nominal parameter value in Table 2 and k_j^* represents the time varying estimate of k_j.

All the kinetic parameters present in the first-order bulk moment equations also appear in the first subsystem. To maintain the triangular structure on which the model decomposition is based, estimated parameters other than rate constants must be introduced into the second subsystem for bias reduction. Several investigators [13,16] have proposed the addition of non-stationary variables to the state equations as an alternative to the use of physically based parameters. For complex systems such as the Tennessee Eastman challenge process [34], proper placement of these non-stationary variables can be quite difficult. An advantage of the proposed model decomposition is that the second subsystem has the same number of state variables and measured variables. This structure allows the introduction of a non-stationary variable to each of the three first-order moment equations as reflected in the second subsystem model (9) where the non-stationary variables are denoted θ_2.

3.3. Estimator formulation

The extended Kalman filter (EKF) [12,24] involves linearization of the nonlinear model at the current estimates followed by application of the linear Kalman filter to the linearized model. Consider the first subsystem (8) in which the four measurements are sampled but undelayed. Define the augmented state vector $z_1 = [\,x_1^{\mathrm{T}} \quad \theta_1^{\mathrm{T}}\,]^{\mathrm{T}}$ and the composite function $\phi_1(z_1, u) = [\,f_1^{\mathrm{T}}(z_1, u) \quad 0^{\mathrm{T}}\,]^{\mathrm{T}}$. A first-order EKF which neglects the second- and higher-order terms of the Taylor series expansion of the nonlinear function $f_1(\cdot)$ is constructed as follows:

- Prediction:

$$\hat{z}_1(kh_1 + h_1|kh_1) = \hat{z}_1(kh_1|kh_1) + \int_{kh_1}^{kh_1+h_1} \phi_1[\hat{z}_1(kh_1|kh_1), u(\tau)]\,\mathrm{d}\tau \tag{11}$$

- Correction:

$$\hat{z}_1(kh_1+h_1|kh_1+h_1) = \hat{z}_1(kh_1+h_1|kh_1) + L_1(kh_1+h_1)[y_1(kh_1+h_1) - C_1\hat{z}_1(kh_1+h_1|kh_1)] \quad (12)$$

where $\hat{z}_1(kh_1+h_1|kh_1)$ denotes the estimated state vector at time kh_1+h_1 from information available at time kh_1. The prediction is performed with constant $\hat{z}_1$ because the first subsystem estimates remain constant over the sampling period h_1. The estimator gain $L_1(kh_1+h_1)$ is calculated from the following recursive equations:

$$L_1(kh_1) = P_1(kh_1|kh_1-h_1)\Psi^{\mathrm{T}}(kh_1) \times [\Psi_1(kh_1)P_1(kh_1|kh_1-h_1)\Psi^{\mathrm{T}}(kh_1)+R]^{-1} \quad (13)$$

$$P_1(kh_1|kh_1) = [I - L_1(kh_1)\Psi(kh_1)]P_1(kh_1|kh_1-h_1) \quad (14)$$

$$P_1(kh_1+h_1|kh_1) = \Phi_1(kh_1)P_1(kh_1|kh_1)\Phi_1^{\mathrm{T}}(kh_1)+Q \quad (15)$$

$$P(0|0) = Q_0 \quad (16)$$

where P_1 is the time varying covariance matrix of the estimated state vector $\hat{z}$, and Q_0, Q and R are constant covariance matrices of the initial state $\hat{x}(0)$, the state disturbance vector, and the measurement noise vector, respectively. The matrices Φ_1 and Ψ_2 are obtained by linearization of the model equations at each sampling instant:

$$\Phi_1(kh_1) = \left[\frac{\partial\phi_1(z_1,u)}{\partial z_1}\right]_{z_1=\hat{z}_1(kh_1|kh_1),u=u(kh_1)}$$
$$\Psi_1(kh_1) = \left[\frac{\partial h_1(z_1)}{\partial z_1}\right]_{z_1=\hat{z}_1(kh_1|kh_1)} \quad (17)$$

The covariance matrices Q_0, Q and R usually are taken to be diagonal and used for estimator tuning. Augmentation of the state vector introduces new elements into the covariance matrices that can be tuned to reduce bias in the estimates of key state variables.

The state and parameter estimates $\hat{z}_1$ from the first subsystem EKF act as inputs to the second subsystem (9). The presence of the time delay t_2 in the three laboratory measurements makes the formulation of the EKF for the second subsystem more complex than that for the first subsystem. Let the augmented state vector z_2 and the composite nonlinear function $\phi_2(z_1,z_2,u)$ be defined analogously to z_1 and $\phi_1(z_1,u)$ respectively. Rather than estimate the current state variables directly, the delayed measurements are used to estimate the state variables one time delay in the past: $z_2(kh_2-t_2|kh_2)$ [10,28]. Then the current estimate $z_2(kh_2|kh_2)$ is generated by open-loop integration of the model (9) with the past estimate as the initial condition. The corresponding prediction and correction equations are:

- One sampling period ahead prediction:

$$\hat{z}_2(kh_2+h_2-t_2|kh_2) = \hat{z}_2(kh_2-t_2|kh_2) + \int_{kh_2-t_2}^{kh_2+h_2-t_2}\phi_2[\hat{z}_1(\tau|kh_2),\hat{z}_2(kh_2-t_2|kh_2),u(\tau)]\,\mathrm{d}\tau \quad (18)$$

- Model correction:

$$\hat{z}_2(kh_2+h_2-t_2|kh_2+h_2) = \hat{z}_2(kh_2+h_2-t_2|kh_2) + L_2(kh_2+h_2)\{y_2(kh_2+h_2) - h_2[\hat{z}_1(kh_2+h_2-t_2|kh_2),\hat{z}_2(kh_2+h_2-t_2|kh_2)]\} \quad (19)$$

- One time delay ahead prediction:

$$\hat{z}_2(kh_2|kh_2) = \hat{z}_2(kh_2-t_2|kh_2) + \int_{kh_2-t_2}^{kh_2}\phi_2[\hat{z}_1(\tau|kh_2),\hat{z}_2(\tau|kh_2),u(\tau)]\,\mathrm{d}\tau \quad (20)$$

The one sampling period ahead prediction is performed with constant $\hat{z}_2$ because the second subsystem estimates remain constant over the sampling period h_2. By contrast, the estimates $\hat{z}_1$ are updated each time the first subsystem EKF is executed. Recursive equations analogous to Eqs. (13)–(16) are used to compute the estimator gain $L_2(kh_2+h_2)$. The time varying matrices Φ_2 and Ψ_2 required in these calculations are obtained by linearization of the second subsystem model equations using expressions analogous to (17).

4. Results and discussion

The performance of the hierarchical EKF is evaluated using the sequence of feed flow rate changes shown in Table 3. The changes represent deviations from a set of nominal feed flow rates. A constant molar ratio of the catalyst (C_1) and co-catalyst (Al) is maintained by treating the ratio of the two molar flow rates as a single input variable. To validate the assumption that the polydispersity remains approximately constant under dynamic conditions, the input sequence is applied to the open-loop reactor model. Although not shown here for the sake of brevity, the results demonstrate that the polydispersity has a maximum deviation of approximately 3% from the steady-state value of two.

EKF performance is evaluated with and without measurement noise for the following cases:

Table 3
Plant input sequence

Feed	M_1 (h)	M_2 (h)	M_3 (h)	C_1, Al (h)	H_2 (h)
−25% step change	0.5	2	3.5	5	6.5
+50% step change	1	2.5	4	5.5	7
−25% step change	1.5	3	4.5	6	7.5

1. *Perfect model*: the EKF design model and the plant model are identical.
2. *Parametric mismatch*: constant parameter bias is introduced by adding zero mean normally distributed errors to the plant kinetic parameters to generate the design model kinetic parameters.
3. *Structural mismatch*: a plant model based upon a different kinetic mechanism than the design model is used.

The EKF covariance matrices are chosen to be diagonal and tuned by trial-and-error for each case to achieve an acceptable tradeoff between dynamic tracking of plant state variables, rejection of measurement noise and minimization of steady-state estimation bias. Estimator performance is highly dependent on the covariance matrices Q and R, while the effect of the Q_0 matrix is negligible. The presence of measurement noise requires the diagonal elements of the R matrix to be increased as compared to noise-free tuning and produces slower estimator convergence due to the smaller measurement correction. EKF performance also is highly dependent on tuning of the covariance matrix elements associated with the adjustable kinetic parameters and the non-stationary variables.

Table 4 shows the covariance matrices for each of the six scenarios investigated. The perfect model and parametric mismatch cases do not require a different set of tuning parameters when measurement noise is introduced, while two different sets of tuning parameters are necessary for the structural mismatch case. The state estimates are initialized to zero, the kinetic parameter

Table 4
EKF tuning parameters

Matrix	Subsystem	Variable	Perfect model		Parametric mismatch		Structural mismatch	
			Noise free	With noise	Noise free	With noise	Noise free	With noise
Q_0	First	All	1.0E−2	1.0E−2	1.0E−2	1.0E−2	1.0E−2	1.0E−2
	Second	All	1.0E−3	1.0E−3	1.0E−3	1.0E−3	1.0E−3	1.0E−3
Q	First	C_{M1}	1.0E+1	1.0E+1	1.0E−11	1.0E−11	1.0E+1	1.0E−3
		C_{M2}	1.0E+1	1.0E+1	1.0E−10	1.0E−10	1.0E+1	1.0E−3
		C_{M3}	1.0E+3	1.0E+3	1.0E−10	1.0E−10	1.0E+3	1.0E−1
		C_{C1}	1.0E−7	1.0E−7	1.0E−14	1.0E−14	1.0E−7	1.0E−11
		C_{C2}	1.0E−7	1.0E−7	1.0E−14	1.0E−14	1.0E−7	1.0E−11
		H_2	1.0E−5	1.0E−5	1.0E−14	1.0E−14	1.0E−5	1.0E−9
		Al	1.0E+3	1.0E+3	1.0E−10	1.0E−10	1.0E+3	1.0E−1
		P_0	1.0E−6	1.0E−6	1.0E−9	1.0E−9	1.0E−6	1.0E−10
		Q_0	1.0E−7	1.0E−7	1.0E−12	1.0E−12	1.0E−7	1.0E−11
		R_0	1.0E−8	1.0E−8	1.0E−14	1.0E−14	1.0E−8	1.0E−12
		B_0	1.0E−5	1.0E−5	1.0E−10	1.0E−10	1.0E−5	1.0E−9
		s_a	0.E0	0.E0	1.0E+4	1.0E+4	1.0E+5	1.0E+3
		s_{11}	0.E0	0.E0	1.0E+4	1.0E+4	1.0E+5	1.0E+3
		s_{13}	0.E0	0.E0	1.0E+3	1.0E+3	1.0E+4	1.0E+2
		s_{tr1}	0.E0	0.E0	1.0E+3	1.0E+3	1.0E+4	1.0E+2
	Second	λ_{100}	1.0E+8	1.0E+8	1.0E−5	1.0E−5	1.0E−4	1.0E−4
		λ_{010}	1.0E+7	1.0E+7	1.0E−5	1.0E−5	1.0E0	1.0E0
		λ_{001}	1.0E+6	1.0E+6	1.0E−5	1.0E−5	1.0E+6	1.0E+6
		d_{100}	0.E0	0.E0	1.0E+5	1.0E+5	1.0E+7	1.0E+7
		d_{010}	0.E0	0.E0	1.0E+5	1.0E+5	1.0E+7	1.0E+7
		d_{001}	0.E0	0.E0	1.0E+5	1.0E+5	1.0E+7	1.0E+7
R	First	C_{M1}	1.0E+6	1.0E+6	1.0E+6	1.0E+6	1.0E−1	1.0E+6
		C_{M2}	1.0E+6	1.0E+6	1.0E+6	1.0E+6	1.0E−1	1.0E+6
		C_{M3}	1.0E+5	1.0E+5	1.0E+6	1.0E+6	1.0E−2	1.0E+5
		λ_0	1.0E+5	1.0E+5	1.0E+7	1.0E+7	1.0E−2	1.0E+5
	Second	$\overline{M}_n$	1.0E0	1.0E0	1.0E+17	1.0E+17	1.0E+17	1.0E+17
		X_{M1}	1.0E+4	1.0E+4	1.0E+17	1.0E+17	1.0E+17	1.0E+17
		X_{M3}	1.0E+2	1.0E+2	1.0E+17	1.0E+17	1.0E+17	1.0E+17

estimates associated with the first subsystem are initialized to unity and the non-stationary parameter estimates associated with the second subsystem are initialized to zero. Estimated concentrations are set to a very small positive value if they become negative to avoid EKF divergence.

4.1. Perfect model

The EKF design model and the plant model are assumed to be identical to investigate the limits of EKF performance. For this set of tests on-line parameter estimation is not necessary and only state estimation is performed. Figs. 1 and 2 show the EKF performance obtained for the plant inputs in Table 3 in the presence of measurement noise implemented as follows:

$$\tilde{y}_i(k) = [1 + r_i n(k)] y_i(k) \tag{21}$$

where y_i is a noise-free plant value, $\tilde{y}_i$ is the noise corrupted plant measurement, n is a zero mean white noise signal, and r_i is scaling parameter used to obtain the desired variance. The scaling parameter r_i is chosen as 0.05 for on-line measurements and 0.02 for laboratory measurements.

Due to the availability of frequent and undelayed on-line measurements, excellent tracking of the first subsystem plant variables is observed despite poor estimator initialization and significant measurement noise (Fig. 1). The second subsystem plant variables are not tracked as effectively because laboratory analysis leads to infrequent and delayed measurement feedback (Fig. 2). Despite the lack of plant information, the EKF is able to quickly converge from the poor initial condition and accurately track the plant variables. The estimate of the number average molecular weight is generally more accurate than the two monomer content estimates. Although not shown here, EKF performance is improved only slightly by the complete removal of measurement noise.

4.2. Parametric mismatch

For the second set of simulation tests the EKF design model is structurally identical to the plant model but random errors in the non-zero kinetic parameters are introduced as follows:

$$\tilde{\theta}_j = (1 + rn)\theta_j \tag{22}$$

where θ_j is a plant parameter, n is a random variable taken from a Gaussian distribution with zero mean and unity variance, $r = 0.1$ is a scaling factor for the variance, and $\tilde{\theta}_j$ is the perturbed parameter used in the design model. Introduction of these random perturbations is intended to mimic uncertainties in the kinetic model parameters that invariably exist even if the model structure is well characterized. On-line parameter estimation is used to minimize bias caused by errors in the 14 non-zero kinetic parameters. Because only four kinetic parameters ($k_a, k_{tr1}, k_{13}, k_{11}$) are adjusted, complete elimination of bias is not possible.

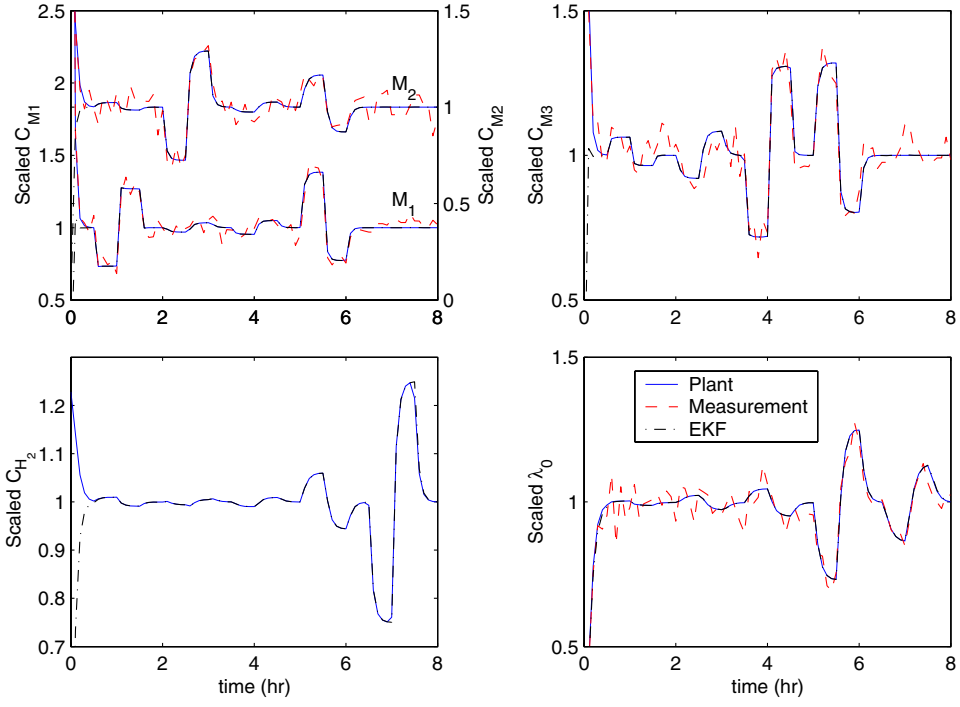

Fig. 1. First subsystem EKF for perfect model with measurement noise.

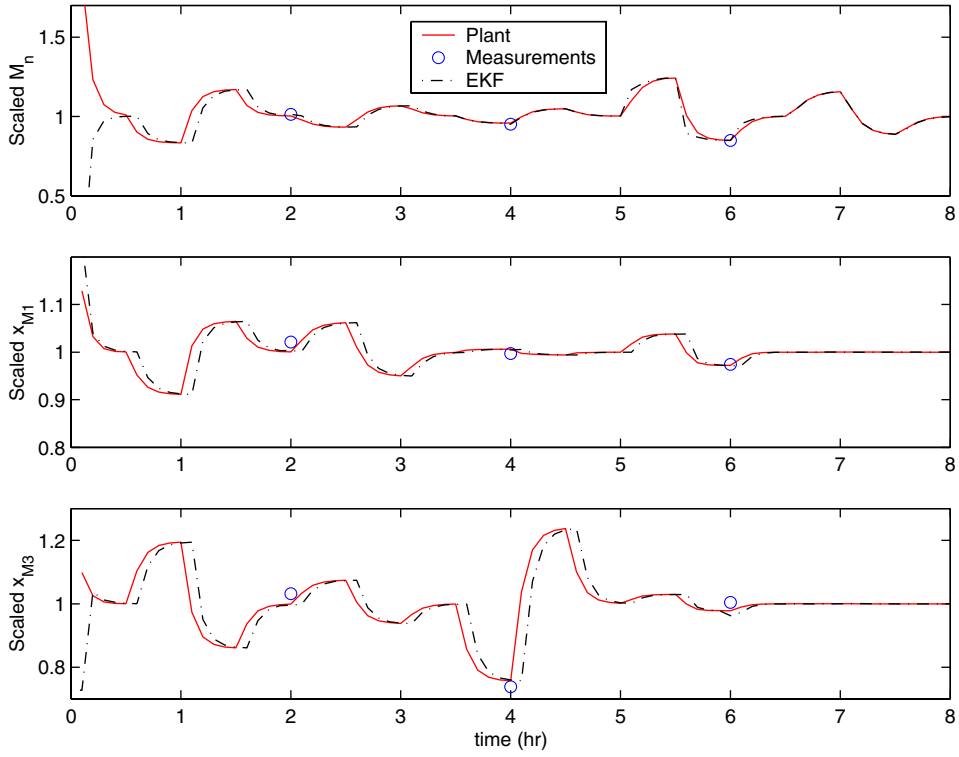

Fig. 2. Second subsystem EKF for perfect model with measurement noise.

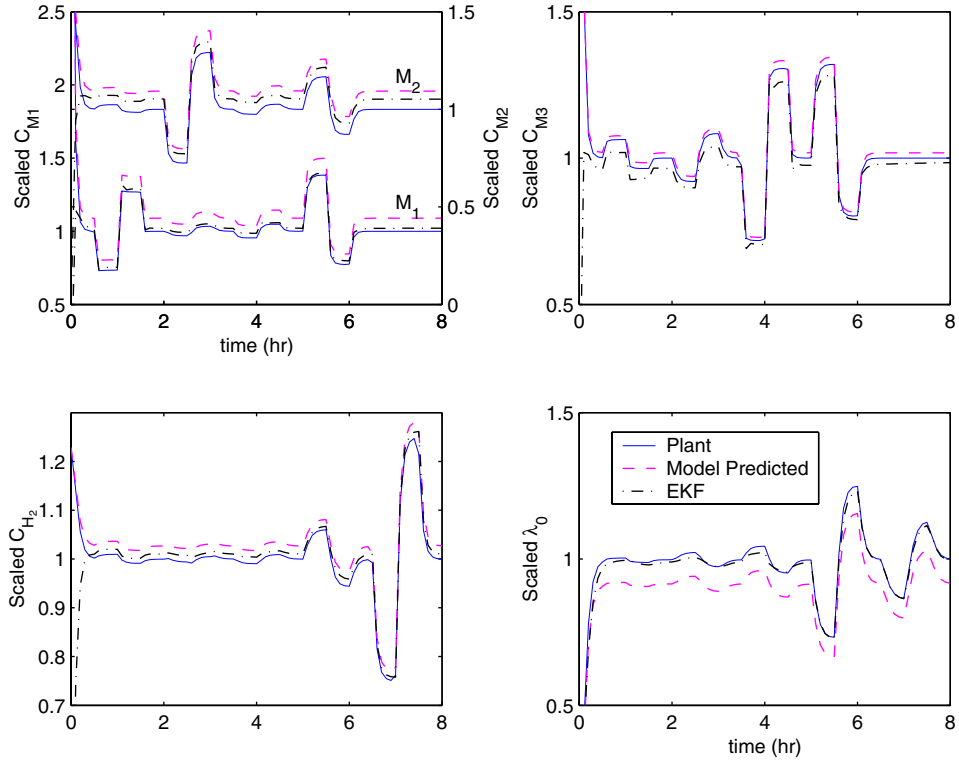

Fig. 3. First subsystem EKF for parametric mismatch without measurement noise.

Figs. 3–5 show the EKF performance obtained in the absence of measurement noise. State estimates obtained from an open-loop observer when the estimates are initialized to zero also are included. While lacking

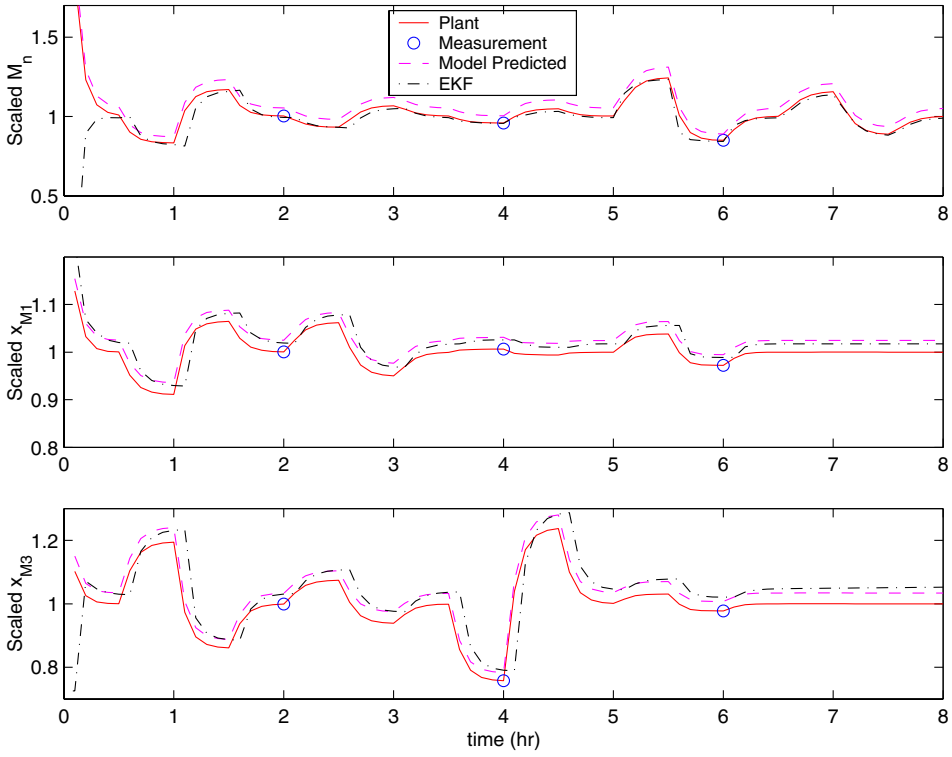

Fig. 4. Second subsystem EKF for parametric mismatch without measurement noise.

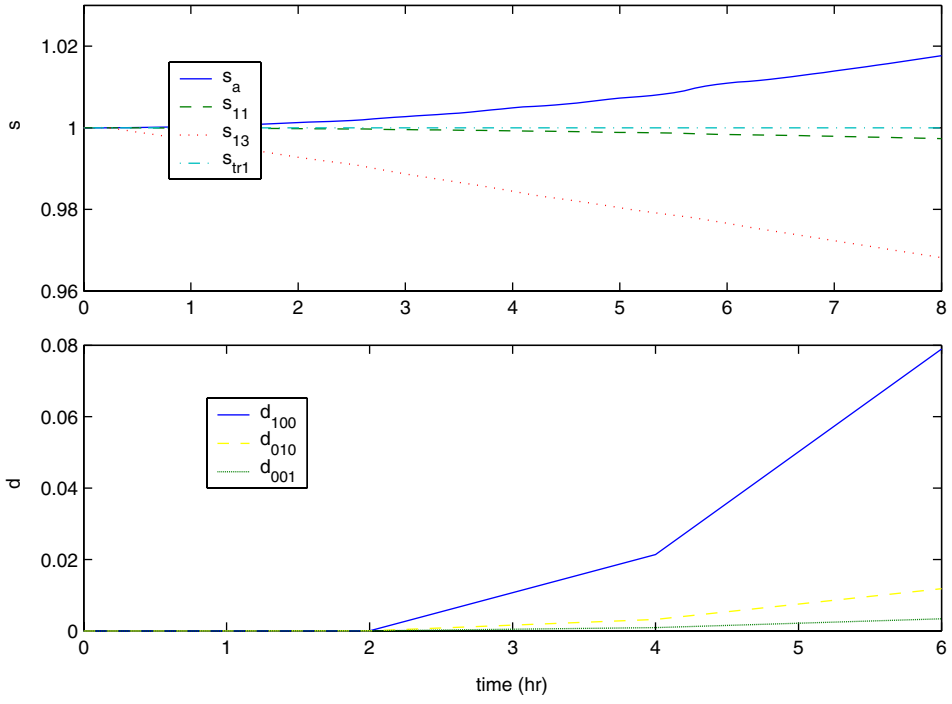

Fig. 5. Estimated parameters for parametric mismatch without measurement noise.

measurement feedback to compensate for plant/model mismatch, the open-loop observer is a reasonable basis for comparison because industrial practitioners often view open-loop estimation as the first alternative for

generating unmeasured state variables. The EKF estimates of the first subsystem variables exhibit slightly faster dynamics and reduced bias as compared to the open-loop estimates (Fig. 3). The improvement is most significant for the ethylene concentration (C_{M_1}) and the total polymer concentration (λ_0). Due to infrequent and delayed measurement feedback, the EKF and open-loop estimates for the second subsystem variables are comparable (Fig. 4).

The evolution of the EKF parameter estimates is shown in Fig. 5. Although not apparent from these plots, all the estimates eventually converge to constant values. Relatively large adjustments in the parameters for catalyst activation (s_a) and diene addition to ethylene ended chains (s_{13}) are required to reduce bias in λ_0 and the diene concentration (C_{M_3}), respectively. The relatively large adjustment in the non-stationary variable d_{100} associated with the second subsystem leads to significant improvements in the estimation of the number average molecular weight ($\overline{M}_n$) as compared to the open-loop observer. Although not shown here, EKF performance is not significantly degraded by the introduction of measurement noise.

4.3. Structural mismatch

In the final set of simulations the plant model is based on a proprietary kinetic mechanism that differs from the mechanism in Table 1 used to derive the EKF design model. These tests are intended to evaluate EKF performance in the presence of substantial plant/model mismatch expected in an industrial application. Figs. 6–8 provide a comparison of EKF and open-loop estimator performance in the absence of measurement noise. Fig. 6 shows that frequent and undelayed measurement feedback allows the EKF to provide superior estimates of the first subsystem variables. The two estimators yield similar performance for the second subsystem because the advantage of feedback is greatly diminished when the plant measurements are available infrequently and with large delay (Fig. 7). The evolution of the EKF parameter estimates is shown in Fig. 8. As compared to the parametric mismatch case (Fig. 5), the EKF produces larger changes in the kinetic parameter for hydrogen chain transfer (s_{tr_1}) and the three non-stationary variables associated with the second subsystem.

EKF performance in the presence of structural mismatch and measurement noise is shown in Figs. 9 and 10. The noise variance parameter r_i in (21) is chosen as 0.05 for on-line measurements and 0.02 for laboratory measurements. As shown in the last two columns of Table 4, the EKF covariance matrices are retuned from their noise-free values. Table 5 provides a comparison of integral square errors for the two estimators. As shown in Fig. 9, the EKF provides superior estimates of the first subsystem state variables including the active catalyst concentration (C_{C_2}) that is very important for

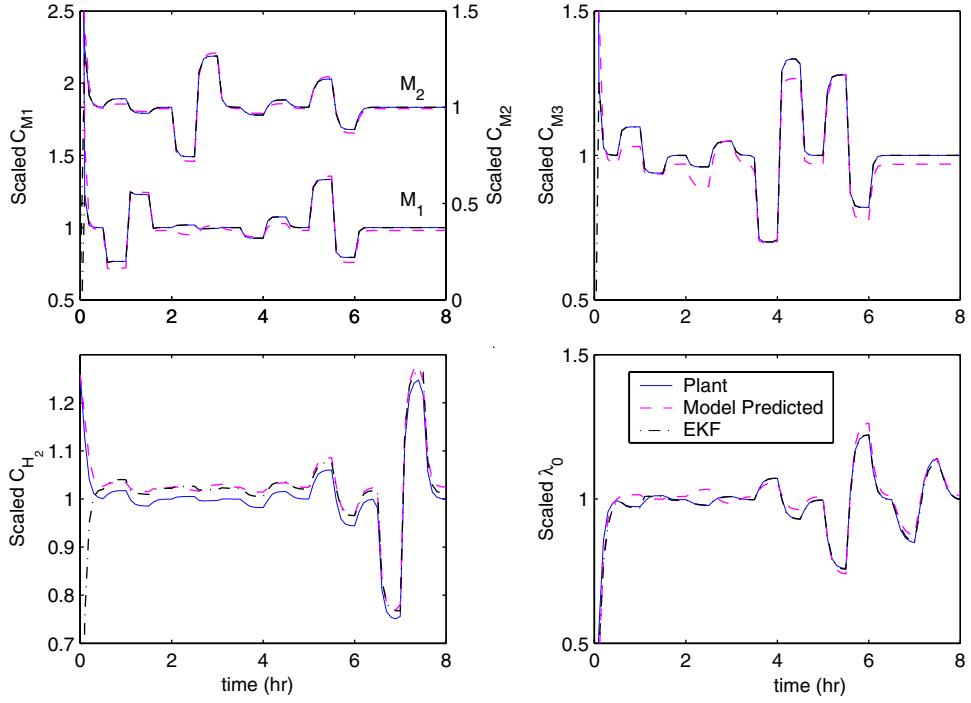

Fig. 6. First subsystem EKF for structural mismatch without measurement noise.

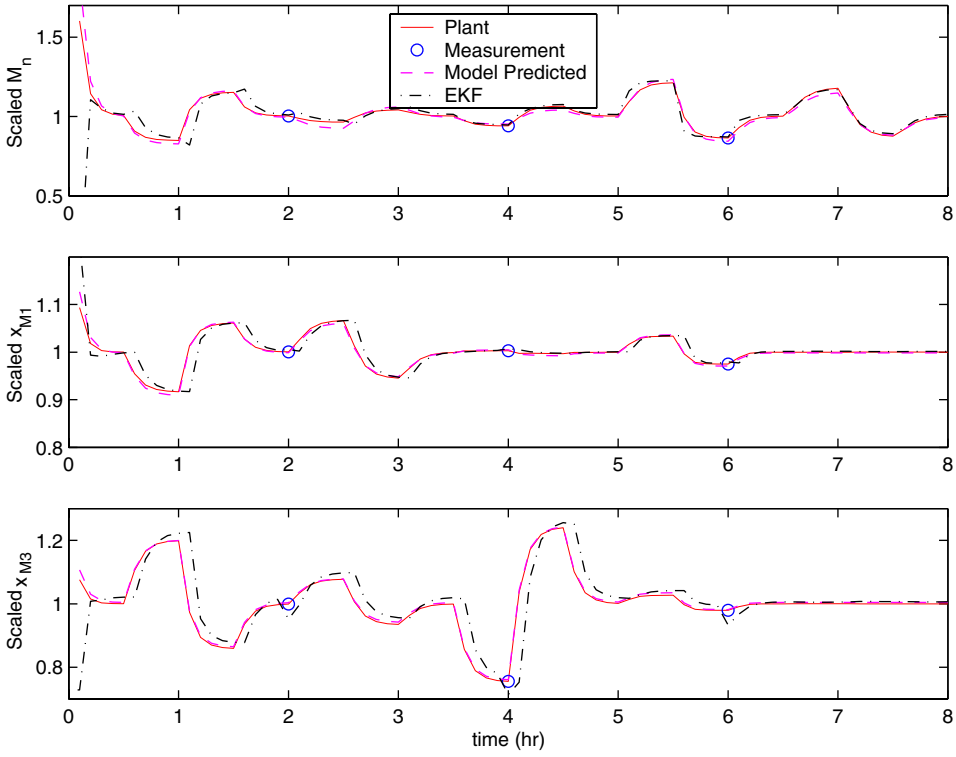

Fig. 7. Second subsystem EKF for structural mismatch without measurement noise.

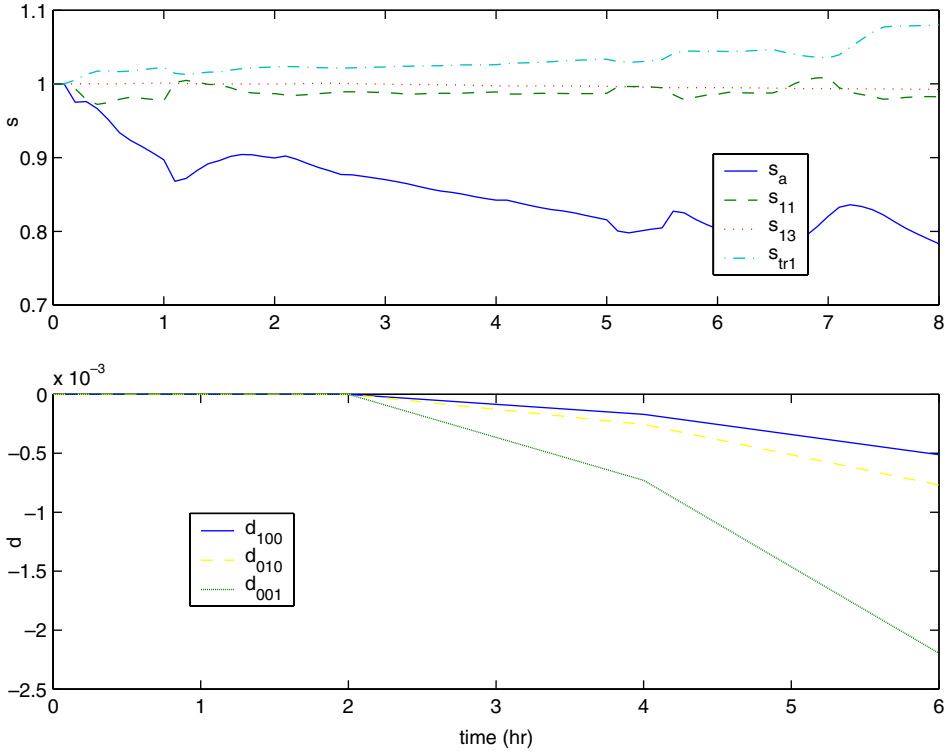

Fig. 8. Estimated parameters for structural mismatch without measurement noise.

production rate control. On-line adjustment of the four kinetic parameters allows the EKF to eliminate estimation bias in the first subsystem measurements. By contrast, the EKF provides comparatively poor esti-

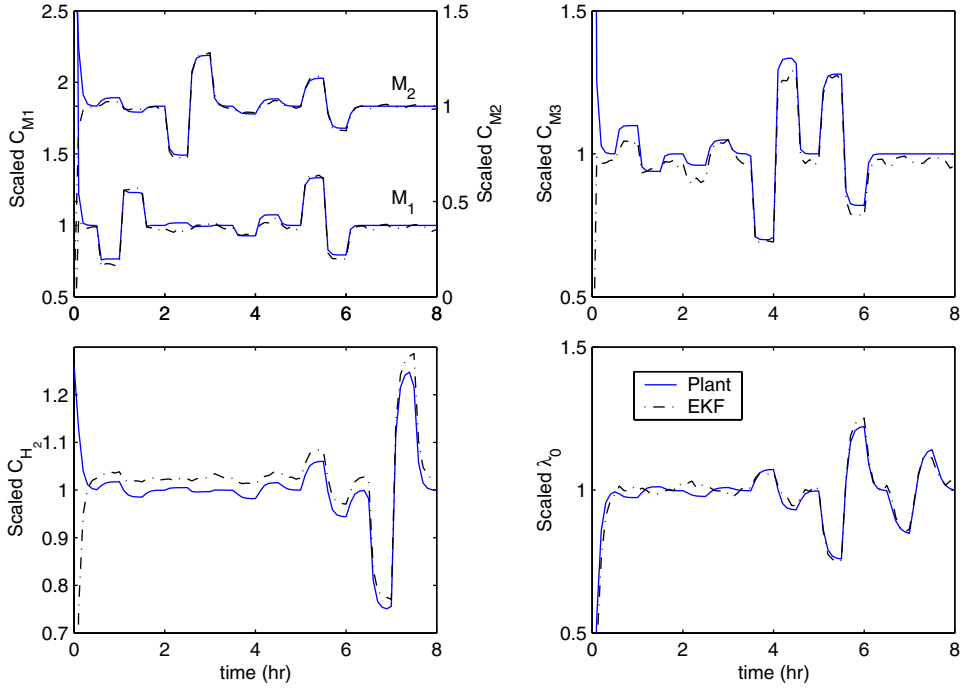

Fig. 9. First subsystem EKF for structural mismatch with measurement noise.

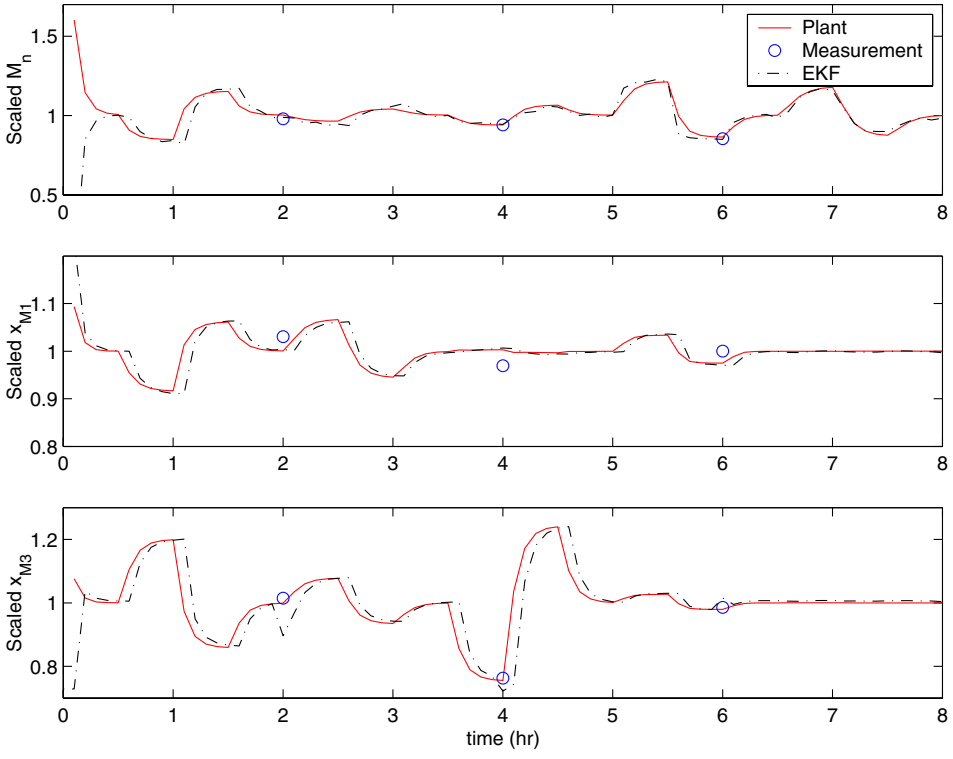

Fig. 10. Second subsystem EKF for structural mismatch with measurement noise.

mates of the second subsystem state variables. Although not shown here, the retuned covariance matrices lead to large changes in the non-stationary variables compared to the noise-free case. As a result, the EKF actually provides better tracking of the polymer product properties than the open-loop estimator (Fig. 10).

Table 5
Integral square estimation errors for structural mismatch with measurement noise

Estimator	C_{M_1}	C_{M_2}	C_{M_3}	C_{C_1}	C_{C_2}	C_{H_2}	C_{Al}
Open-loop	4.65	6.00E−1	5.70	3.16E+1	3.23E+1	2.20E−1	1.72E−1
EKF	3.10	3.80E−1	4.42	3.20E+1	2.53E+1	2.12E−1	1.71E−1
Estimator	P_0	Q_0	R_0	B_0	λ_{100}	λ_{010}	λ_{001}
Open-loop	3.84E+1	3.31E+1	2.65E+1	4.43	2.12E−1	1.18E−1	4.91E−1
EKF	2.95E+1	2.37E+1	1.95E+1	2.03	1.68	1.79	4.78

5. Summary and conclusions

A hierarchical extended Kalman filter (EKF) design based on a first principles model of a continuous ethylene–propylene–diene polymer reactor was presented. The dynamic model is decomposed into two subsystems by exploiting the triangular model structure and the different sampling frequencies of the available on-line and laboratory measurements. The first subsystem is comprised of differential equations for the reactant concentrations and the zeroth-order moments of the molecular weight distribution (MWD). An augmented version of the first subsystem is used to design an EKF that generates estimates of unmeasured state variables and four kinetic parameters from on-line measurements of the ethylene, propylene, diene and total polymer concentrations. The second subsystem consists of first-order MWD moment equations in which the state variables of the first subsystem represent unknown inputs. A hierarchical design in which estimates of the first subsystem variables serve as inputs to an EKF designed for the second subsystem has been developed. The second subsystem EKF generates frequent estimates of the polymer contents and number average molecular weight from infrequent and delayed laboratory measurements of these quantities. The proposed formulation allows the second subsystem correction term to be utilized only when laboratory measurements become available.

The hierarchical EKF differs from existing multirate estimation techniques in which on-line and laboratory measurements are integrated into a single estimator designed using the complete reactor model. While these other techniques are potentially applicable to the EPDM problem, the proposed method offers several advantages including reduced computational requirements, improved numerical stability, easier implementation and reduced maintenance. A variety of simulation tests involving measurement noise, parametric modeling errors and structural plant/model mismatch were used to evaluate the hierarchical estimation strategy. The results show that the EKF provides effective tracking of reactant and polymer concentrations, while infrequent and delayed laboratory measurement feedback limits the accuracy of the polymer property estimates. The proposed design strategy is applicable to other types of polymerization reactors with on-line measurements of reactant concentrations and laboratory measurements correlated to higher-order MWD moments.

Acknowledgements

Financial support from the ExxonMobil Chemical Company is gratefully acknowledged.

Appendix A

A.1. EPDM reactor model

Reactant concentration equations

$$\frac{dC_{M_1}}{dt} = \frac{F}{V}(C_{M_{1,f}} - C_{M_1}) - (k_{i1}C_{C_2} + k_{11}P_0 + k_{21}Q_0 + k_{31}R_0)C_{M_1} \quad (A.1)$$

$$\frac{dC_{M_2}}{dt} = \frac{F}{V}(C_{M_{2,f}} - C_{M_2}) - [k_{i2}C_{C_2} + k_{12}P_0 + k_{22}Q_0 + (k_{t_2} + k_{tr_{M_2}})(P_0 + Q_0 + R_0)]C_{M_2} \quad (A.2)$$

$$\frac{dC_{M_3}}{dt} = \frac{F}{V}(C_{M_{3,f}} - C_{M_3}) - [(k_{x_3}C_{C_2} + k_{13}P_0 + k_{t_3}(P_0 + Q_0 + R_0)]C_{M_3} \quad (A.3)$$

$$\frac{dC_{C_1}}{dt} = \frac{F}{V}(C_{C_{1,f}} - C_{C_1}) - (k_a + k_x + k_{x_3}C_{M_3})C_{C_1} \quad (A.4)$$

$$\frac{dC_{C_2}}{dt} = -\frac{F}{V}C_{C_2} + [k_aC_{C_1} - (k_{i1}C_{M_1} + k_{i2}C_{M_2})C_{C_2} + k_{tr_1}C_{H_2}(P_0 + Q_0 + R_0)] \quad (A.5)$$

$$\frac{dC_{Al}}{dt} = \frac{F}{V}(C_{Al,f} - C_{Al}) - k_{tr}\left(\frac{C_{Al}}{C_{C_1}} - 1\right)(P_0 + Q_0 + R_0) \quad (A.6)$$

$$\frac{dC_{H_2}}{dt} = \frac{F}{V}(C_{H_{2,f}} - C_{H_2}) - k_{tr_1}C_{H_2}(P_0 + Q_0 + R_0) \quad (A.7)$$

Zeroth-order moment equations

$$\frac{dP_0}{dt} = -\frac{F}{V}P_0 + k_{i1}C_{C_2}C_{M_1} + (k_{21}Q_0 + k_{31}R_0)C_{M_1} - (k_{12}C_{M_2} + k_{13}C_{M_3})P_0 - (k_t + k_{t_2}C_{M_2} + k_{t_3}C_{M_3} + k_{tr_1}C_{H_2} + k_{tr_{M_2}}C_{M_2})P_0 + k_{tr}\left(\frac{C_{Al}}{C_{C_1}} - 1\right)(Q_0 + R_0) \quad (A.8)$$

$$\frac{dQ_0}{dt} = -\frac{F}{V}Q_0 + k_{i2}C_{C_2}C_{M_2} + k_{12}C_{M_2}P_0 - k_{21}C_{M_1}Q_0 - \left[k_t + k_{t_2}C_{M_2} + k_{t_3}C_{M_3} + k_{tr_1}C_{H_2} + k_{tr}\left(\frac{C_{Al}}{C_{C_1}} - 1\right)\right]Q_0 + k_{tr_{M_2}}C_{M_2}(P_0 + R_0) \quad (A.9)$$

$$\frac{dR_0}{dt} = -\frac{F}{V}R_0 + k_{13}C_{M_3}P_0 - k_{31}C_{M_1}R_0 - \left[k_t + k_{t_2}C_{M_2} + k_{t_3}C_{M_3} + k_{tr_1}C_{H_2} + k_{tr}\left(\frac{C_{Al}}{C_{C_1}} - 1\right) + k_{tr_{M_2}}C_{M_2}\right]R_0 \quad (A.10)$$

$$\frac{dB_0}{dt} = -\frac{F}{V}B_0 + \left[k_t + k_{t_2}C_{M_2} + k_{t_3}C_{M_3} + k_{tr_1}C_{H_2} + k_{tr}\left(\frac{C_{Al}}{C_{C_1}} - 1\right) + k_{tr_{M_2}}C_{M_2}\right]\cdot(P_0 + Q_0 + R_0) \quad (A.11)$$

First-order moment equations

$$\frac{d\lambda_{100}}{dt} = -\frac{F}{V}\lambda_{100} + k_{i1}C_{C_2}C_{M_1} + (k_{11}P_0 + k_{21}Q_0 + k_{31}R_0)C_{M_1} + k_{tr}\left(\frac{C_{Al}}{C_{C_1}} - 1\right)P_0 \quad (A.12)$$

$$\frac{d\lambda_{010}}{dt} = -\frac{F}{V}\lambda_{010} + (k_{i2}C_{C_2} + k_{12}P_0 + k_{22}Q_0)C_{M_2} + k_{tr_{M_2}}C_{M_2}Q_0 \quad (A.13)$$

$$\frac{d\lambda_{001}}{dt} = -\frac{F}{V}\lambda_{001} + k_{13}C_{M_3}P_0 \quad (A.14)$$

A.2. Kinetic parameter selection algorithm

The EPDM kinetic parameters selected for on-line estimation are determined using the following recursive algorithm [17]:

1. Consider a steady-state operating point of the reactor model denoted as $\bar{u}$, $\bar{x}$, $\bar{y}$ and $\bar{\theta}$. Introduce a small perturbation $\Delta\theta_j = \theta_j - \bar{\theta}_j$ in the jth non-zero kinetic parameter and denote the steady-state change in the ith output as $\Delta y_i = y_i - \bar{y}_i$. Compute the dimensionless sensitivity coefficient matrix $\tilde{S} = \{\tilde{S}_{ij}\}$:
$$\tilde{S}_{ij} = \frac{\Delta y_i/\bar{y}_i}{\Delta\theta_j/\bar{\theta}_j} \quad (A.15)$$
2. Perform principal component analysis [8] on the covariance matrix $X = \tilde{S}^{\mathrm{T}}\tilde{S}$. Denote $m = 4$ as the number of measured outputs and $\lambda \in R^m$ as the vector of non-zero eigenvalues of X. Compute the overall effect metric $E_j \in [0,1]$ of the jth parameter:
$$E_j = \frac{\sum_{i=1}^{m}|\lambda_i C_{ij}|}{\sum_{i=1}^{m}|\lambda_i|} \quad (A.16)$$
where C_{ij} represents an element of the principal component matrix. Select the highest ranked parameter $p_1 = \{\theta_k | E_k = \max_j E_j\}$, and set the number of selected parameters $n = 1$.
3. Compute the linear independence metric $d_j \in [0,1]$ for each parameter θ_j not already selected:
$$d_j = \sin\left[\cos^{-1}\left(\frac{\tilde{s}_j^{\mathrm{T}}\tilde{s}}{\|\tilde{s}_j\|\|\tilde{s}\|}\right)\right] \quad (A.17)$$
where $\tilde{s}_j$ is the dimensionless sensitivity vector associated with θ_j, and $\tilde{s}$ is the vector in the space spanned by the sensitivity vectors of the parameters $\{p_1, \ldots, p_n\}$ previously chosen for estimation which is closest to $\tilde{s}_j$ in the Euclidean sense [17].
4. Calculate the identifiability metric $I_j \in [0,1]$ for each parameter θ_j not already selected:
$$I_j = E_j d_j \quad (A.18)$$
Select the next highest ranked parameter $p_{n+1} = \{\theta_k | I_k = \max_j I_j\}$, and set the number of selected parameters $n = n + 1$. If $n < m$, then return to step 3. Otherwise, terminate the algorithm.

References

[1] Hazardous air pollutant emissions from process units in the elastomer manufacturing industry—Basis and purpose document for proposed standards. Technical Report EPA-453/R-95-006a, Office of Air Quality, Environmental Protection Agency, May 1995.

[2] D.K. Adebekun, F.J. Schork, Continuous solution polymerization reactor control. 2. Estimation and nonlinear reference control during methyl methacrylate polymerization, Ind. Eng. Chem. Res. 28 (1989) 1846–1861.

[3] J. Alvarez, T. Lopez, Robust dynamic state estimation of nonlinear plants, AIChE J. 45 (1999) 107–123.

[4] J.S. Baras, A. Bensoussan, M.R. James, Dynamic observers as asymptotic limits of recursive filters: Special cases, SIAM J. Appl. Math. 48 (1988) 1147–1158.

[5] G. Bastin, M.R. Gevers, Stable adaptive observers for nonlinear time-varying systems, IEEE Trans. Autom. Control, AC 33 (1988) 650–658.

[6] C. Cozewith, Transient response of continuous-flow stirred-tank polymerization reactors, AIChE J. 34 (1988) 272–282.

[7] C. Cozewith, G.W. Ver Strate, Ethylene–propylene copolymers reactivity ratios, evaluation, and significance, Macromolecules 4 (1971) 482–489.

[8] G.H. Dunteman, Principal Components Analysis, Sage Publications, Newbury Park, CA, 1989.

[9] E.K. Easterbrook, R.D. Allen, Ethylene–propylene rubber, in: M. Morton (Ed.), Rubber Technology, Chapter 9, Van Nostrand Reinhold, New York, NY, 1987, pp. 260–283.

[10] M.F. Ellis, T.W. Taylor, V. Gonzales, K.F. Jensen, Estimation of molecular weight distribution in batch polymerization, AIChE J. 34 (1988) 1341–1353.

[11] A. Gelb, Applied Optimal Estimation, MIT Press, Cambridge, MA, 1974.

[12] A.H. Jazwinski, Stochastic Processes and Filtering Theory, Academic Press, New York, NY, 1970.
[13] D.J. Kozub, J.F. MacGregor, State estimation for semi-batch polymerization reactors, Chem. Eng. Sci. 47 (1992) 1047–1062.
[14] A.J. Krener, A. Isidori, Linearization by output injection and nonlinear observers, System Control Lett. 3 (1983) 47–52.
[15] M.J. Kurtz, G.-Y. Zhu, M.A. Henson, Constrained output feedback control of a multivariable polymerization reactor, IEEE Trans. Control Systems Tech. 8 (2000) 87–97.
[16] J.H. Lee, N.L. Ricker, Extended Kalman filter based nonlinear model predictive control, Ind. Eng. Chem. Res. 33 (1994) 1530–1541.
[17] R. Li, M.A. Henson, M.J. Kurtz, Selection of model parameters for off-line parameter estimation, IEEE Trans. Control Systems Tech., in press.
[18] L. Ljung, Asymptotic behavior of the extended Kalman filter as a parameter estimator for linear systems, IEEE Trans. Autom. Control 24 (1979) 36–50.
[19] K.B. McAuley, J.F. MacGregor, Nonlinear product property control in industrial gas-phase polyethylene reactors, AIChE J. 39 (1993) 855–866.
[20] N.G. McCrum, C.P. Buckley, C.B. Bucknall, Principles of Polymer Engineering, second ed., Oxford University Press, Oxford, UK, 1998.
[21] M.F. McDonald, R.L. Long, C.J. Thomas, On-line control of a chemical process plant, US Patent 6,072,576, June 6, 2000.
[22] H. Michalska, D.Q. Mayne, Moving horizon observers and observer-based control, IEEE Trans. Autom. Control 40 (1995) 995–1006.
[23] P.E. Moraal, J.W. Grizzle, Observer design for nonlinear systems with discrete-time measurements, IEEE Trans. Autom. Control AC 40 (1995) 395–404.
[24] K.R. Muske, T.F. Edgar, Nonlinear state estimation, in: M.A. Henson, D.E. Seborg (Eds.), Nonlinear Process Control, Chapter 6, Prentice-Hall, Englewood Cliffs, NJ, 1997, pp. 311–370.
[25] R.K. Mutha, W.R. Cluett, A. Penlidis, On-line model-based estimation and control of a polymer reactor, AIChE J. 43 (1997) 3042–3058.
[26] B.A. Ogunnaike, On-line modelling and predictive control of an industrial terpolymerization reactor, Int. J. Control 59 (1994) 711–729.
[27] M.J. Park, S.M. Hur, H.K. Rhee, On-line estimation and control of polymer quality in a reactor, AIChE J. 48 (2002) 1013–1021.
[28] V. Prasad, M. Schley, L.P. Russo, B.W. Bequette, Product property and production rate control of styrene polymerization, J. Process Control 12 (2002) 353–372.
[29] C.V. Rao, J.B. Rawlings, Nonlinear moving horizon estimation, in: F. Allgower, A. Zheng (Eds.), Nonlinear Model Predictive Control, Birkhauser, Basel, 2000, pp. 45–69.
[30] C.V. Rao, J.B. Rawlings, D.Q. Mayne, Constrained state estimation for nonlinear discrete-time systems: stability and moving horizon approximations, IEEE Trans. Autom. Control 48 (2003) 246–258.
[31] W.H. Ray, On the mathematical modeling of polymerization reactors, J. Macromol. Sci.-Revs. Macromol. Chem. C 8 (1972) 1–56.
[32] K. Reif, S. Gunther, E. Yaz, R. Unbehauen, Stochastic stability of the discrete-time extended Kalman filter, IEEE Trans. Autom. Control 44 (1999) 714–728.
[33] K. Reif, R. Unbehauen, The extended Kalman filter as an exponential observer for nonlinear systems, IEEE Trans. Signal Process. 47 (1999) 2324–2328.
[34] N.L. Ricker, J.H. Lee, Nonlinear modeling and state estimation for the Tennessee Eastman challenge process, Comput. Chem. Eng. 19 (1995) 983–1005.
[35] C.A. Sandink, K.B. McAuley, P.J. McLellan, Selection of parameters for updating in on-line models, Ind. Eng. Chem. Res. 40 (2001) 3936–3950.
[36] A. Sirohi, K.Y. Choi, On-line parameter estimation in a continuous polymerization process, Ind. Eng. Chem. Res. 35 (1996) 1332–1343.
[37] G. Ver Strate, Ethylene–propylene elastomers, in: Encyclopedia of Polymer Science and Engineering, Wiley, New York, NY, 1986, pp. 522–564.
[38] S. Tatiraju, M. Soroush, Nonlinear state estimation in a polymerization reactor, Ind. Eng. Chem. Res. 36 (1997) 2679–2690.
[39] S. Tatiraju, M. Soroush, B.A. Ogunnaike, Multirate nonlinear state estimation with application to a polymerization reactor, AIChE J. 45 (1999) 769–780.
[40] M. van Dootingh, F. Viel, D. Rakotopara, J.P. Gauthier, P. Hobbes, Nonlinear deterministic observer for state estimation: application to a continuous free radical polymerization reactor, Comput. Chem. Eng. 16 (1992) 777–791.
[41] M. Zeitz, The extended Luenberger observer for nonlinear systems, System Control Lett. 9 (1987) 149–156.